THE ASTROPHYSICAL JOURNAL, 290:735–741, 1985 March 15

MULTIFREQUENCY RADIO VLBI OBSERVATIONS OF THE SUPERLUMINAL, LOW-FREQUENCY VARIABLE QUASAR NRAO 140

ALAN P. MARSCHER
Department of Astronomy, Boston University

AND

JOHN J. BRODERICK
Department of Physics, Virginia Polytechnic Institute and State University
Received 1983 November 3; accepted 1984 September 20

ABSTRACT

We present VLBI maps of the quasar NRAO 140 at three wavelengths: 18, 6, and 2.8 cm. The source consists of a jetlike structure delineated by a nearly colinear series of components which are progressively more compact toward the northwestern end of the source. The multifrequency observations allow us to dissect accurately the spectrum of the source, which leads to an affirmation of the previously reported Compton problem and superluminal motion. The Compton problem requires relativistic motion with Doppler factor $\delta > 3.7$. One of the components is separating from the "core" at a rate of 0.15 milliarcsec yr^{-1}, which translates to an apparent velocity between $4c$ and $13c$, depending on the values of H_0 and q_0. The energy in relativistic electrons in one of the components far exceeds the energy in magnetic field, but the total energy requirement need not exceed $\sim 10^{54}$ ergs.

Subject headings: interferometry — quasars — radio sources: variable

I. INTRODUCTION

In a previous pair of papers on the $z = 1.258$ quasar NRAO 140 (Marscher and Broderick 1981*a*, *b*), we used VLBI observations at 2.8 cm both to determine angular sizes and to dissect the total radio spectrum into its individual components. We found that this source has a "Compton problem" in that the X-ray flux predicted by standard synchrotron theory far exceeds that observed. The only solution to this Compton problem is for at least one of the radio components to be moving relativistically at a small angle to the line of sight. As opposed to other indicators of relativistic motion, this result is independent of the distance to the source. Since relativistic motion is also thought to be the cause of the superluminal motions observed in a number of compact radio sources (for recent reviews, see Kellermann and Pauliny-Toth 1981; Cohen and Unwin 1982, 1983), one would expect that NRAO 140 would also exhibit superluminal motion. Subsequent observations (Marscher and Broderick 1982, hereafter Paper II) yielded a preliminary confirmation that superluminal motion does indeed occur in this source, as predicted.

In addition to the above behavior at high radio frequencies, the source is a low-frequency variable (Dennison *et al.* 1981; Fanti *et al.* 1981; Dennison *et al.* 1984), with an implied brightness temperature (see Jones and Burbidge 1973) between 5×10^{15} K ($H_0 = 50$ km s^{-1} Mpc^{-1}, $q_0 = 0$) and 5×10^{14} K ($H_0 = 100$, $q_0 = 1$), where the angular size is obtained from the variability time scale (see Jones, O'Dell, and Stein 1974; Burbidge, Jones, and O'Dell 1974) and a cosmological interpretation of the redshift using a standard Friedmann cosmology. If the brightness changes are intrinsic to the source (which may not be the case; see Rickett, Coles, and Bourgois 1984), this again leads to a Compton problem (excessive predicted Compton X-ray flux, short Compton lifetimes of the relativistic electrons, or both).

There are two basic reasons why this research on NRAO 140 has been important to the study of compact extragalactic radio sources. First, the distance-independent conclusion that relativistic motion must be occurring in the source and the observation of superluminal motion together suggest that relativistic motion is in fact the correct explanation of the superluminal phenomenon. None of the other models for superluminal motion also solves the Compton problem. Second, NRAO 140 is the first object which has been observed to both vary at low frequencies and undergo superluminal motion. Although relativistic motion has been the leading hypothesis for explaining both phenomena, this source is the first which has been observed to display all of the expected ramifications of the relativistic effects.

Since NRAO 140 plays such a crucial role in the understanding of compact radio sources, it is extremely important that we confirm that the above results are in fact correct. For example, the dissection of the radio spectrum was based solely on 2.8 cm VLBI observations and the total flux density at various wavelengths. It was assumed that the individual components have spectra characteristic of incoherent synchrotron sources. It is much more reliable to use VLBI observations at several wavelengths, since these explicitly yield the flux densities of the individual components. In addition, the superluminal motion observed (Paper II) involved an increase in separation which amounted to less than 50% of the extent of the component. Hence, the possibility remained that brightness changes within the component, rather than component motion, caused the shift in the position of the brightness centroid.

Here we describe the results of further VLBI observations of NRAO 140 at wavelengths of 18, 6, and 2.8 cm. These observations confirm the existence of a Compton problem in NRAO 140 and confirm that one of the components is separating from the "core" at a superluminal velocity.

II. OBSERVATIONS

We observed NRAO 140 at 18 cm on 1981 October 9 using a six-element VLB array consisting of the 100 m telescope at

Effelsburg, West Germany (referred to as "BONN"); the 37 m antenna of Haystack Observatory (HSTK) near Westford, Massachusetts; the 43 m dish at the National Radio Astronomy Observatory[1] (NRAO) in Green Bank, West Virginia; the 26 m dish at Harvard Radio Astronomy Station in Fort Davis, Texas; the 40 m antenna of Owens Valley Radio Observatory (OVRO) near Big Pine, California; and the 26 m antenna at Hat Creek (HCRK), California. We also observed it at 2.8 cm on 1982 October 2 using the same array, and at 6 cm on 1981 August 17 using BONN, HSTK, FDVS, and OVRO. Processing of the video tapes and subsequent data analysis were performed at Caltech using the JPL-CIT processor and VAX computer, as well as the VLBI software developed by the CIT–JPL staff, most notably T. J. Pearson. Total flux density measurements were obtained at BONN (R. Porcas, private communication). System temperature calibrations were made each hour at all stations, as were antenna temperature calibrations at BONN and NRAO. For the remaining stations, predetermined gain curves of antenna temperature versus zenith angle were used. Our final calibration of correlated flux densities is estimated to be self-consistent at the 5% level at 18 and 2.8 cm and at the 10% level at 6 cm. We obtained final high dynamic-range maps for the six-station 1981 October (18 cm) and 1982 October (2.8 cm) experiments by using the self-calibration routine AMPHI written by S. C. Unwin after the method of Cornwell and Wilkinson (1981).

III. RESULTS

a) 18 Centimeter Observations

Our 18 cm data are of sufficient quality to generate a hybrid map (Readhead and Wilkinson 1978) of NRAO 140 with a dynamic range of ~50:1. The map is presented in Figure 1. The hybrid map model provides an excellent fit to both the amplitude and closure phase data (not shown). Since the source structure is extended mainly along position angle 130°, we find it useful to also present in Figure 2*a* a map which has been smoothed by a circular Gaussian of FWHM = 3.0 milliarcseconds (mas). This is equivalent to the effective resolution *along the position angle of the source axis, 130°*. Our north-south resolution is not this high, so the map can only be used to determine the positions of the components and their extents along P.A. = 130°. The source is essentially unresolved perpendicular to the source axis. Three components, each somewhat elongated in about the same direction as that of the source axis, show up clearly on the map. As our 6 and 2.8 cm observations indicate, the bright, northwestern component actually consists of two components, A and B, separated by ~2 mas.

[1] NRAO is operated by Associated Universities, Inc., under contract with the National Science Foundation.

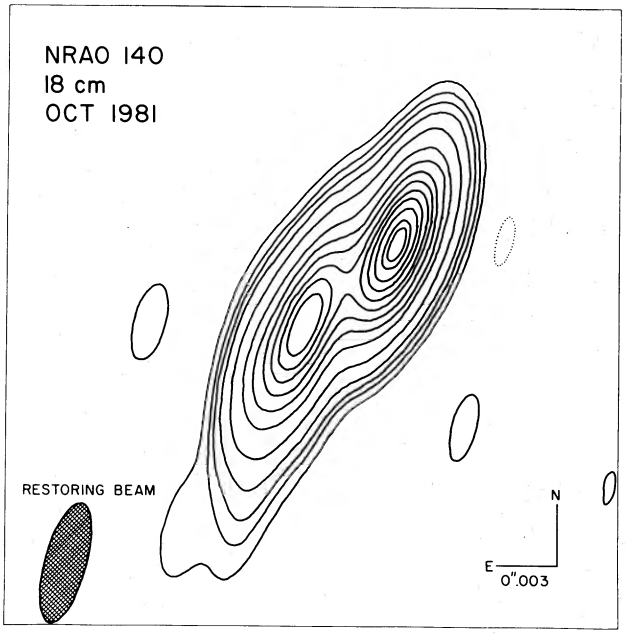

FIG. 1.—Hybrid map of NRAO 140 at 18 cm at epoch 1981 October. Contour levels are −0.4%, 1%, 2%, 3%, 5%, 10%, 30%, 50%, 70%, and 90% of peak brightness of 4.1×10^{10} K.

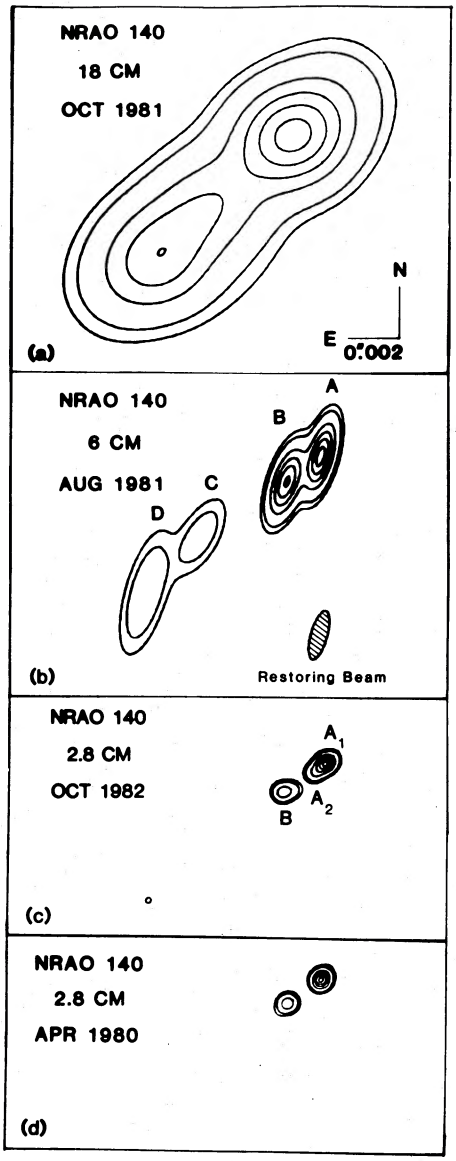

FIG. 2.—Hybrid maps (*a*, *c*, *d*) and model (*b*) at the wavelengths and epochs indicated on the figures. Scale indicated in (*a*) and component identifications given in (*b*) apply to all maps. Contour levels are 5%, 10%, 30%, 50%, 70%, and 90% of peak brightness. Peak brightness temperatures are (*a*) 5.5×10^{10} K, (*b*) 3.0×10^{10} K, (*c*) 4.4×10^{10} K, and (*d*) 5.4×10^{10} K. Restoring beam is indicated in (*b*). Maps (*a*), (*c*), and (*d*) were smoothed with circular Gaussians of FWHM 3.0, 0.5, and 0.5 mas, respectively.

To the southeast lie two more components, C and D, separated by ~4 and 8 mas, respectively, from the blended A/B component. Together, the components define a knotty jet, with a length-to-width ratio greater than ~4:1. The total flux density of the source is 3.03 ± 0.05 Jy, whereas the total flux density of components A, B, C, and D is 2.90 Jy. About 5% of the flux density therefore comes from low surface brightness regions. At least some of this arises in two weak extended lobes observed with conventional interferometers at P.A. = 149° relative to the core (Schilizzi and de Bruyn 1983; Browne *et al.* 1982; Perley 1982). Our hybrid map model (see Fig. 1) indicates the presence of a 0.08 Jy component located 15 mas from component A/B at P.A. = 145° at the 3% brightness contour. Also, the 1% contour indicates that a still weaker component may also be present at the southeast tip of the source. Although this latter component is below the dynamic range of the map, we have recently obtained a 100:1 dynamic-range map (epoch 1984 April) which confirms its existence. It is interesting that both these weak components, as well as the more extended lobes, are misaligned with the inner jet. All lie at larger position angles than the inner jet, but the penultimate VLBI component lies at a significantly larger position angle than does the outermost one.

b) 6 Centimeter Observations

Because a receiver failure at NRAO restricted our array to four stations, the data are not sufficient to yield a high-quality hybrid map. This results mainly from the deficit of short baselines. Nevertheless, a crude (dynamic range of ~5:1) hybrid map was constructed to use as a guide to model fitting. A starting model consisting of four components was used, based on this hybrid map plus our previous 2.8 cm observations (Marscher and Broderick 1981*b*; hereafter Paper I) for components A and B, and our 18 cm observations for components C and D. Subsequent iterations adjusted the relative positions, flux densities, and sizes of the components until a final model was produced which yielded excellent agreement with the data (agreement factor is equivalent to the square root of the reduced χ^2 function, equal to 0.8 for both amplitudes and closure phases). The model source (smoothed with an elliptical Gaussian beam) is shown in Figure 2*b*. While the relative positions of the various components are reliable, the directions of elongation and sizes are probably not. Components C and D are not well defined owing to the lack of short baselines: the maximum correlated flux density is 1.9 Jy (on the HSTK–FDVS baseline), compared to a total flux density of 2.7 Jy. Hence, their sizes and relative flux densities are quite uncertain at 6 cm.

c) 2.8 Centimeter Observations

We obtained 2.8 cm observations in 1982 October with two purposes in mind: to confirm the preliminary indication of superluminal motion and to obtain a high-quality map. The map is needed to determine whether there are any features in the low-level structure which would have led us to erroneous component angular sizes determined by model-fitting our 1980 April data (Paper I). As is the case at 18 cm, the data are of extremely high quality, which has allowed us to obtain a hybrid map with a dynamic range of ~30:1. The resultant map is presented in Figure 3, smoothed with an elliptical Gaussian beam indicative of the resolution at various position angles. Figure 2*c* shows the same map, smoothed with a circular Gaussian beam of FWHM = 0.5 mas, the effective resolution

FIG. 3.—Hybrid map of NRAO 140 at 2.8 cm at epoch 1982 October. Contour levels are −1%, 2%, 3%, 5%, 10%, 30%, 50%, 70%, and 90% of peak brightness of 2.1×10^{10} K.

along the source axis (P.A. ≈ 130°). In order to facilitate comparison with our original 1980 April observations, a hybrid map representing NRAO 140 at this earlier epoch is given in Figure 2*d*; here the data are also smoothed with a circular Gaussian beam of FWHM = 0.5 mas.

The map shows that the source has beome more complicated since our first observations in 1980 April. (This is most clearly seen by comparing Figs. 2*c* and 2*d*.) Component A, which was only very slightly resolved in 1980, now possesses an extension to the southeast, along essentially the same position angle as the other components. The earlier suspicion (Paper II) that component A consists of two subcomponents is therefore borne out.

Notice that component C is resolved out at the 5% level, while component D is just barely visible. Even component D does not appear above the 5% contour level on our 1980 April map (Fig. 2*d*), since these observations did not employ the short OVRO–HCRK baseline.

d) Overall Structure of NRAO 140

By combining these multifrequency observations, along with our earlier 2.8 cm observations, we are able to synthesize a coherent picture of the structure of NRAO 140. As is the case with many other sources, the basic morphology of NRAO 140 consists of an extremely compact (angular extent less than ~0.2 mas) core (the northeast portion of component A, hereafter referred to as A1), out of which emanates a lumpy jet composed of several nearly colinear components (B, C, and D as given in Fig. 2*b*, plus the southwestern portion of A, which we hereafter designate A2). The general trend is for the components farther from the core to be more extended. There is no evidence for any counterjet given the present dynamic range of the maps.

It is possible for us to obtain a reasonably accurate dissection of the centimeter wavelength spectrum of NRAO 140 using our multifrequency VLBI maps. The main obstacles are the insensitivity of our 6 and 2.8 cm data to components C and D, and the blending of components A and B at 18 cm. The former problem leads to rather large errors in determining the 6 and 2.8 cm flux densities of components C and D. The latter problem, however, can be tackled as follows. Components A and B are separated by 1.8 mas as indicated by our shorter wavelength maps. This is 0.6 times our FWHM resolution along the structural axis, so A and B are not completely blended at 18 cm. This is illustrated by the elliptical shape of the A/B component in Figure 2*a*. So the placement of the hybrid map δ-functions gives some indication of the relative flux densities of components A and B. A second method is to assume that the separation of component D from component B at 6 and 2.8 cm is about the same as that at 18 cm. (Spectral gradients are assumed to be weak or nonexistent. We expect this to hold since component D is optically thin at 18 cm and component B is too small to have a dominant effect on the separation.) This assumption allows us to position component B relative to D, after which the relative flux densities of components A and B can be adjusted until the position of the centroid of A/B matches that observed (again, relative to component D). Both methods yield identical results: the flux density of component B is ~ 2.9 times that of component A at 18 cm.

Table 1 lists our determination of the parameters of each component as observed at 1981.7 ± 0.1. We interpolate the 2.8 cm parameters between our 1981 June and 1982 October observations. The extremely slow variability ($\lesssim 0.1$ Jy per year in total flux density and little change in structure other than positional shifts) of NRAO 140 at 2.8 cm allows us to do this with confidence. Figure 4 shows the radio spectrum from 0.1 to 15 GHz, and indicates the contributions from the individual components. The curves representing the individual components are extrapolations at frequencies below 1.66 GHz. Comparison of Figure 4 with Figure 4 of Paper I indicates that the preliminary spectrum of Paper I was quite close to the actual spectrum, except that we underestimated the 2–6 GHz flux density of component B in order to minimize the expected Compton flux. (That is, the most "conservative" spectral decomposition was drawn in order to show that the existence of a Compton problem was a necessary consequence of the observations.) Although there was about a 1.5 yr time lag between our 1980 April observations and our 1981.7 observations, NRAO 140 varied by no more than ~ 0.1 Jy at any wavelength between 1.4 and 8 GHz during this period. So there is little likelihood that the spectral decomposition given in Figure 4 does not also represent that at epoch 1980 April, at least to a good approximation. Note also from Figures 2*c* and 2*d* that the angular size of component B has not changed noticeably (except for a possible small increase in extent along P.A. $\approx -70°$) between 1980 April and 1982 October, so that the spectrum of component B is unlikely to have evolved appreciably owing to expansion or contraction.

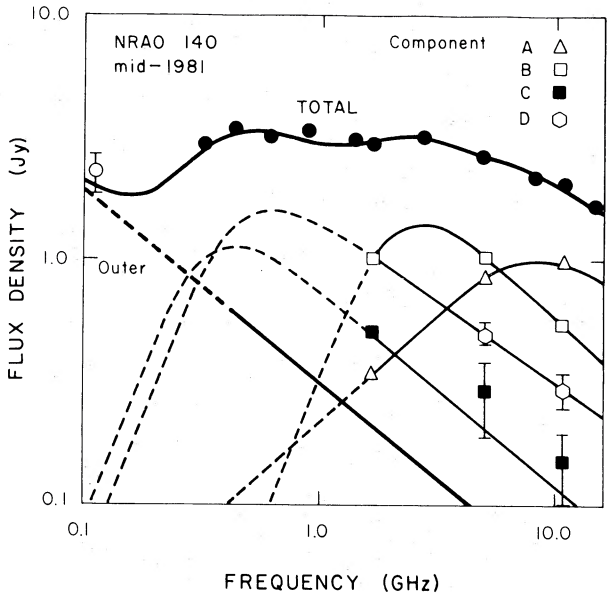

FIG. 4.—Radio spectrum of NRAO 140. Sources of data are as follows. This work: 1.66, 5, and 10.7 GHz. Dent (private communication): 2.7 GHz. Aller and Aller (private communication): 8.0 and 15.5 GHz. Dennison *et al.* (1984): 0.318–1.40 GHz. 1972 ± 1 data from Clark *et al.* (1975): 0.111 GHz. Decomposition of spectrum into individual components is indicated; dashed curves indicate extrapolations. Solid curve represents sum of individual component contributions. Errors of data without error bars are approximately given by the sizes of the symbols. Data point at 1.67 cm for component D coincides with that given for component B.

The spectrum of the "outer" components includes the flux density from compact sources other than A, B, C, or D, which are present in our 18 cm observation (as indicated by the maximum correlated flux density), but beyond the dynamic range of the map, plus the extended structure detected by Schilizzi and de Bruyn (1983), Perley (1982), and Browne *et al.* (1982). A spectral index $\alpha = 0.75$ (defined such that the flux density at frequency ν is $S_\nu \propto \nu^{-\alpha}$) fits the spectrum of the extended ("outer") components, and is assumed to also apply approximately to component C, whose spectrum is poorly determined.

Determination of the angular sizes of the compact components is an important but difficult undertaking, owing not

TABLE 1

PROPERTIES OF RADIO COMPONENTS OF NRAO 140 IN MID-1981

COMPONENT	FLUX DENSITIES (Jy) 2.8 cm	6 cm	18 cm	SEPARATION FROM A1 (mas)	POSITION ANGLE OF SEPARATION	FWHM MAJOR AXIS (mas)	MINOR/MAJOR AXIAL RATIO
A_1 }	1.0 ± 0.05	0.87 ± 0.05	0.35 ± 0.05	...	...	<0.2	...
A_2 }				~0.45	131° ± 5°	<0.2	...
B	0.55 ± 0.05	1.04 ± 0.05	1.01 ± 0.05	1.8 ± 0.05	126° ± 3°	0.41[a]	0.65[a]
C	0.15 ± 0.05	0.29 ± 0.1	0.51 ± 0.03	5.7 ± 0.5	130° ± 3°	~2.6	≲0.8
D	0.30 ± 0.05	0.51 ± 0.05	1.02 ± 0.03	8.6 ± 0.5	132° ± 3°	~2	~1

[a] Established from our 1980 April observations; see text.

only to the limited resolution, but also, in the cases of components C and D, to the lack of sensitivity to the less compact structure at 6 and 2.8 cm. Components A1 and A2 are unresolved even at 2.8 cm, which limits their angular extents to less than ~ 0.2 mas. Component B is partially resolved at 2.8 cm. However, the complication of the emergence of subcomponent A2 makes it difficult to determine a unique angular size for component B at epoch 1982 October by using model-fitting routines. Because of this, only rather weak upper limits could be placed on the angular size if these were the only data to which we had access. But in 1980 April components A1 and A2 were blended (i.e., their angular separation was unresolved), so that NRAO 140 possessed essentially a simple double structure as seen by the longer baselines. Model fitting *does* yield reliable (to within reasonable expected error) angular sizes of simple doubles. Hence, we can determined the angular extent of component B with confidence for epoch 1980 April, and use the absence of variability (see Figs. 2*c* and 2*d*) to argue that this determination also holds to a good approximation for epoch 1981.7. This was done by remodeling our 1980 April data taking into account our new knowledge of the geometry of the source (the existence of components C and D, plus the unresolved double nature of component A). The result of this procedure is given in Table 1. One could in theory also obtain the angular size of component B from the hybrid map by deconvolving the beam from the map, but this leads to very uncertain results when the component size is less than that of the beam.

For components C and D, we can obtain rough angular sizes by noting that these components are fully detected on the shortest baselines at 18 cm, and only partially detected on the shortest baselines at 6 and 2.8 cm. Our hybrid map model indicates that component C is only slightly resolved at 18 cm (angular size therefore less than ~ 2 mas), while component D is unresolved perpendicular to the structural axis (P.A. = 130°) but resolved with an angular extent ~ 2.6 mas along this position angle. Our 2.8 and 6 cm data should have been sensitive to structures as large as ~ 2 mas, so we estimate 2 mas to be a reasonable approximation to the angular size of component C and to the angular extent of component D along P.A. $\approx 40°$. We plan to make additional 6 cm observations involving several short baselines in order to determine the dimensions of components C and D more precisely.

IV. DISCUSSION

a) Physical Characteristics and the Compton Problem of NRAO 140

We can use the spectral decomposition and observed angular size of component B to determine the physical parameters of this component (see Paper I; for formulae see Burbidge, Jones, and O'Dell 1974; Marscher 1983). The spectral index α is steeper than assumed in Paper I, and the flux density at the turnover frequency, $S_m = S_\nu(\nu_m)$, larger. Also, the rederived equivalent size θ_s (see Paper I for a definition) of component B is slightly larger than that given in Paper I. The observed parameters which we have determined are $\alpha \approx 0.75$ (α appears to steepen above ~ 6 GHz), $\nu_m = 2.7$ GHz, $S_m = 1.6$ Jy (recall that S_m is obtained from an extrapolation of the high-frequency spectrum), and $\theta_s = 0.6$ mas. Since the spectrum steepens at high frequencies, a reasonable estimate for the effective high-frequency cutoff seems to be $\nu_2 \approx 4\nu_m$. This appears only in a logarithmic factor. For a relativistic Doppler factor (see the above references for a definition) δ, we obtain for the magnetic field

$$B \approx 1 \times 10^{-4}\delta \text{ gauss} .$$

The energy density of relativistic electrons radiating from frequency ν_m to ν_2 can also be calculated. Here we give the relevant formula, which was presented with incorrect numerical factors by Marscher *et al.* (1979). For a source with redshift z and luminosity distance $D_{\rm Gpc}$ gigaparsecs, we find that the energy density is

$$u_{\rm re} = f(a, \nu_m, \nu_2) D_{\rm Gpc}^{-1} \theta_s^{-9} \nu_m^{-7} S_m^4 (1+z)^7 \delta^{-5} \text{ ergs cm}^{-3} . \quad (1)$$

The function f is given by

$$\begin{aligned} f &= 0.95[(\nu_2/\nu_m)^{1/4} - 1] \quad (\alpha = 0.25) , \\ &= 0.27 \ln (\nu_2/\nu_m) \quad (\alpha = 0.50) , \\ &= 0.47[1 - (\nu_m/\nu_2)^{1/4}] \quad (\alpha = 0.75) , \\ &= 0.23[1 - (\nu_m/\nu_2)^{1/2}] \quad (\alpha = 1.00) . \end{aligned}$$

For component B, the (minimum) energy density in relativistic electrons is then

$$u_{\rm re} \approx 2(12.3/D_{\rm Gpc})\delta^{-5} \text{ ergs cm}^{-3} .$$

The quantity $D_{\rm Gpc} = 12.3$ for $H_0 = 50$, $q_0 = 0$, and is lower for higher values of H_0 and q_0. This can be compared with the energy density in magnetic field,

$$u_B \approx 5 \times 10^{-10}\delta^2 \text{ ergs cm}^{-3} .$$

From our estimated uncertainties in the observed parameters (typically $\sim 10\%$), we find that the values given above are accurate to within a factor of ~ 3 for B, and ~ 10 for $u_{\rm re}$ and u_B. Unless the Doppler factor δ is greater than ~ 25, the relativistic electrons dominate the energetics of component B. The total energy in component B is

$$E_{\rm re} \approx 1 \times 10^{58}(D_{\rm Gpc}/12.3)^2\delta^{-5}\Gamma \text{ ergs} ,$$

where Γ is the bulk Lorentz factor of the component (typically, $\Gamma \approx \delta$). If we include the effects of relativistic motion as indicated by the Compton problem and the superluminal motion of component B relative to A1, with $\delta \approx 5$–15, we find that the total energy in this component need not be greater than $\sim 10^{54}$ ergs.

Although the above calculation of the derived energy content of the source argues quite strongly for relativistic motion of component B, the Compton calculation (Paper I) is more definitive. Using the equations given in Marscher (1983), we find that the observable parameters of component B yield an expected Compton X-ray flux density at photon energy 1 keV:

$$S_x \approx 2200\delta^{-5.5} \ \mu\text{Jy} .$$

This can be compared with the observed X-ray flux density of 1.6 μJy (Paper I). The discrepancy can be accounted for if component B is moving relativistically with a Doppler factor

$$\delta > 3.7 .$$

Of course, it is possible (even likely) that the observed X-ray flux contains only a small contribution from component B, in which case the Doppler factor would have to be considerably larger than the above limit.

It was stressed in Paper I that *only* relativistic motion represents a plausible solution to the Compton problem in NRAO 140. This conclusion is independent of distance or the effects of gravitational lenses (since these preserve the observed brightness temperature). Also, component B is partially resolved by our array, so only an extremely unlikely conspiracy of coherent or very high brightness emitters could solve the Compton problem while giving the appearance of an incoherent source. One possible flaw does remain, and that is that we have determined the angular size at a frequency which exceeds the turnover frequency by a factor of 4. It is the size of the source at ν_m which should be plugged into the formulae (Cohen 1983 also briefly discusses this problem). The angular size could depend on frequency because of inhomogeneities (multiple subcomponents or gradients in physical parameters), but this serves only to *increase* the magnitude of the Compton problem in most cases (Marscher 1977). One nonuniformity which *could* affect the size determination in the sense required is a radial gradient in maximum electron energy. The high-energy electrons which radiate at 10.7 GHz might be confined to a smaller volume than the somewhat lower energy electrons which radiate at 2.7 GHz. This possibility conforms with the steep spectrum of component B above 6 GHz. However, synchrotron radiation is fairly broad band, so a deficit of electrons whose radiation peaks at 10.7 GHz also suppresses (albeit to a somewhat lesser extent) the radiation at 2.7 GHz. An independent calculation by one of us (Marscher, in preparation) indicates that, for this reason, it is *not* possible for gradients in maximum electron energy to alleviate significantly the Compton problem.

b) Superluminal Motion in NRAO 140

As discussed in Paper I, the inference that component B is moving relativistically implies that it should also appear to move superluminally when VLBI observations obtained at different epochs are compared. While it is possible for relativistic beaming to occur within an apparently stationary feature (e.g., at the base of a relativistic jet; see Blandford and Königl 1979), the morphology of NRAO 140 is quite similar to those of known superluminal sources (see, e.g., Unwin *et al.* 1983; Walker *et al.* 1982), in which compact components (similar to component B in NRAO 140) appear to separate at superluminal velocities from the core. Our preliminary observations given in Paper II indicated that component B is in fact undergoing superluminal motion.

Comparison of our 1982 October map (Fig. 2*c*) with our 1980 April map (Fig. 2*d*) shows that, if the northwestern portion of component A (A1) is to be identified with the core, component B has indeed moved relative to this core between these epochs. It is possible to contrive a model involving only small component motions. This model requires A2 to have been dominant over A1 in 1980 April, and A2 to have decreased while A1 increased in flux density since then. However, our intermediate 1981 June observations argue against this, since they indicate that the separation of components A1 and A2, as well as that of components B and A1, has increased since that epoch. Also, the interpretation that component A2 represents another "jet" component emerging from the core is consistent with the behavior of other superluminal sources (see Cohen and Unwin 1983 for a review).

In order to determine the separation rate of component B relative to A1, we register the maps obtained at different epochs by lining up the contours at the northwestern edges of component A in Figures 2*c* and 2*d*. This procedure is consistent with the method used for other superluminal sources (see, e.g., Walker *et al.* 1982), but is prone to considerable uncertainty since components A1 and A2 were blended in 1980 April. We therefore also determined the component separations by means of model fitting at each epoch. The hybrid maps yield an increase in separation of 0.36 mas from 1980 April to 1982 October (a time span of 2.48 yr), while the model fitting yields an increase of 0.38 mas during the same period. The fact that both methods yield similar results is reassuring. We therefore determine that the separation of component B from A1 increased by 0.37 ± 0.03 mas in 2.48 yr, which yields an angular separation rate of 0.15 ± 0.01 mas yr^{-1}. For $q_0 = 0$, 1 light-year corresponds to $0.0524\ h^{-1}$ mas, while for $q_0 = 1$, 1 lt-yr corresponds to $0.0855\ h^{-1}$ mas, where $h = H_0/100$ km s^{-1} Mpc^{-1}. We therefore find (after taking into account time dilation) that the apparent separation velocity ranges from $6.5 \pm 0.5\ h^{-1}\ c$ for $q_0 = 0$, to $4.0 \pm 0.4\ h^{-1}\ c$ for $q_0 = 1$. We note that the above separation rate is, within the errors, similar to that obtained in Paper II for 1980 April to 1981 June. It is also consistent with the prediction that the Compton problem requires $\delta > 3.7$ (see above), which implies that the apparent separation rate should exceed $\sim 4c$.

The separation of component B from A1 was 2.0 ± 0.1 mas in 1982 October. At a constant separation rate of 0.15 mas yr^{-1}, the separation of A1 and B would have been zero in early 1969. An isolated peak of a slow outburst at 2.8 cm occurred at this epoch (Andrew *et al.* 1978). A similar isolated outburst began in 1976 and peaked in 1978–1979 (Marscher *et al.* 1979; Balonek 1982). It is tempting to identify the creation of component A2 with this latter event. The 1982 October separation of component A2 from A1 is ~ 0.55 mas, so a separation rate of 0.10 to 0.15 mas yr^{-1} would imply zero separation during the flux density outburst. We plan to continue to monitor NRAO 140 in order to determine whether component A2 is in fact separating from A1 at such a rate.

c) Low-Frequency Variability of NRAO 140

Our 18 cm observation of NRAO 140 happened to coincide with the peak of a flux density outburst at low frequencies, observed by Dennison *et al.* (1984) at frequencies ranging from 0.43 to 0.88 GHz (70–34 cm wavelength). The amplitude of the outburst was $\sim 20\%$ (0.55 Jy) at 34 cm, and less than $\sim 10\%$ at 21 cm. Unless the spectrum of the fluctuating component was *extremely* steep ($\alpha > 3$), it should be present on our 18 cm map. Extrapolation of our spectral dissection (Fig. 4) suggests either component C or D as the likely site of the low-frequency brightness changes. We are in the process of carrying out observations which would test this.

The authors gratefully acknowledge absentee observing support at the observatories used in this study, and the assistance of the Caltech staff (notably G. Dvorak and S. Unwin) during the data reduction process. We also appreciate the communication of data, prior to publication, by W. Dent, T. Balonek, B. Dennison, and N. Bartel. Discussions with M. Cohen, S. Unwin, and B. Dennison proved quite beneficial to this study. Both A. P. M. and J. J. B. were supported in part by the National Science Foundation (NSF). In addition, A. P. M. was partially supported by a Graduate School Seed Grant at Boston University. The NSF also supports radio astronomy at Berkeley (HCRK), Caltech (OVRO), Harvard (FDVS), and Haystack Observatory (HSTK), which is operated by the Northeast Radio Observatory Corporation.

REFERENCES

Andrew, B. H., MacLeod, J. M., Harvey, G. A., and Medd, W. J. 1978, *A.J.*, **83**, 863.
Balonek, T. J. 1982, Ph.D. thesis, University of Massachusetts.
Blandford, R. D., and Königl, A. 1979, *Ap. J.*, **232**, 34.
Browne, I. W. A., Clark, R. R., Moore, P. K., Muxlow, T. W. B., Wilkinson, P. N., Cohen, M. H., and Porcas, R. W. 1982, *Nature*, **299**, 788.
Burbidge, G. R., Jones, T. W., and O'Dell, S. L. 1974, *Ap. J.*, **193**, 43.
Clark, T. A., Erickson, W. C., Hutton, L. K., Resch, G. M., Vandenberg, N. R., Broderick, J. J., Knowles, S. H., and Youmans, A. B. 1975, *A.J.*, **80**, 923.
Cohen, M. H. 1983, in *Proc. Bangalore Winter School on Energetic Extragalactic Sources*, p. 1.
Cohen, M. H., and Unwin, S. C. 1983, in *IAU Symposium 110, VLBI and Compact Radio Sources*, ed. R. Fanti, K. I. Kellerman, and G. Setti (Dordrecht: Reidel), p. 95.
Cornwell, T. J., and Wilkinson, P. N. 1981, *M.N.R.A.S.*, **196**, 1067.
Dennison, B., Broderick, J. J., Ledden, J. E., O'Dell, S. L., and Condon, J. J. 1981, *A.J.*, **86**, 1604.
Dennison, B., Broderick, J. J., O'Dell, S. L., Mitchell, K. J., Altschuler, D. R., Payne, H. E., and Condon, J. J. 1984, *Ap. J. (Letters)*, **281**, L55.
Fanti, C., Fanti, R., Ficarra, A., Mantovani, F., Padrielli, L., and Weiler, K. W. 1981, *Astr. Ap. Suppl.*, **45**, 61.
Jones, T. W., and Burbidge, G. R. 1973, *Ap. J.*, **186**, 791.
Jones, T. W., O'Dell, S. L., and Stein, W. A. 1974, *Ap. J.*, **188**, 353.
Kellermann, K. I., and Pauliny-Toth, I. I. K. 1981, *Ann. Rev. Astr. Ap.*, **19**, 373.
Marscher, A. P. 1977, *Ap. J.*, **216**, 244.
———. 1983, *Ap. J.*, **264**, 296.
Marscher, A. P., and Broderick, J. J. 1981*a*, *Ap. J. (Letters)*, **247**, L49.
———. 1981*b*, *Ap. J.*, **249**, 406 (Paper I).
———. 1982, *Ap. J. (Letters)*, **255**, L11 (Paper II).
Marscher, A. P., Marshall, F. E., Mushotzky, R. F., Dent, W. A., Balonek, T. J., and Hartman, M. F. 1979, *Ap. J.*, **233**, 498.
Perley, R. A. 1982, *A.J.*, **87**, 859.
Readhead, A. C. S., and Wilkinson, P. N. 1978, *Ap. J.*, **223**, 25.
Rickett, B. J., Coles, W. A., and Bourgois, G. 1984, *Astr. Ap.*, **134**, 390.
Schilizzi, R. T., and de Bruyn, A. G. 1983, *Nature*, **303**, 26.
Unwin, S. C., Cohen, M. H., Pearson, T. J., Seielstad, G. A., Simon, R. S., Linfield, R. P., and Walker, R. C. 1983, *Ap. J.*, **271**, 536.
Walker, R. C., Seielstad, G. A., Simon, R. S., Unwin, S. C., Cohen, M. H., Pearson, T. J., and Linfield, R. P. 1982, *Ap. J.*, **257**, 56.

JOHN J. BRODERICK: Department of Physics, VPI & SU, Blacksburg, VA 24061

ALAN P. MARSCHER: Department of Astronomy, Boston University, 725 Commonwealth Ave., Boston, MA 02215